

# Circulation

JOURNAL OF THE AMERICAN HEART ASSOCIATION



## **Effective arterial elastance as index of arterial vascular load in humans**

RP Kelly, CT Ting, TM Yang, CP Liu, WL Maughan, MS Chang and DA Kass  
*Circulation* 1992;86;513-521

Circulation is published by the American Heart Association, 7272 Greenville Avenue, Dallas, TX 72514

Copyright © 1992 American Heart Association. All rights reserved. Print ISSN: 0009-7322. Online ISSN: 1524-4539

The online version of this article, along with updated information and services, is located on the World Wide Web at:

<http://circ.ahajournals.org>

Subscriptions: Information about subscribing to *Circulation* is online at  
<http://circ.ahajournals.org/subscriptions/>

Permissions: Permissions & Rights Desk, Lippincott Williams & Wilkins, a division of Wolters Kluwer Health, 351 West Camden Street, Baltimore, MD 21202-2436. Phone: 410-528-4050. Fax: 410-528-8550. E-mail:  
[journalpermissions@lww.com](mailto:journalpermissions@lww.com)

Reprints: Information about reprints can be found online at  
<http://www.lww.com/reprints>

# Effective Arterial Elastance as Index of Arterial Vascular Load in Humans

Raymond P. Kelly, Chih-Tai Ting, Tsong-Ming Yang, Chung-Peng Liu, W. Lowell Maughan, Mau-Song Chang, and David A. Kass, MD

**Background.** This study tested whether the simple ratio of ventricular end-systolic pressure to stroke volume, known as the effective arterial elastance ( $E_a$ ), provides a valid measure of arterial load in humans with normal and aged hypertensive vasculatures.

**Methods and Results.** Ventricular pressure–volume and invasive aortic pressure and flow were simultaneously determined in 10 subjects (four young normotensive and six older hypertensive). Measurements were obtained at rest, during mechanically reduced preload, and after pharmacological interventions. Two measures of arterial load were compared: One was derived from aortic input impedance and arterial compliance data using an algebraic expression based on a three-element Windkessel model of the arterial system [ $E_a(Z)$ ], and the other was more simply measured as the ratio of ventricular end-systolic pressure to stroke volume [ $E_a(PV)$ ]. Although derived from completely different data sources and despite the simplifying assumptions of  $E_a(PV)$ , both  $E_a(Z)$  and  $E_a(PV)$  were virtually identical over a broad range of altered conditions:  $E_a(PV) = 0.97 \cdot E_a(Z) + 0.17$ ;  $n = 33$ ,  $r^2 = 0.98$ ,  $SEE = 0.09$ ,  $p < 0.0001$ . Whereas  $E_a(PV)$  also correlated with mean arterial resistance, it exceeded resistance by as much as 25% in older hypertensive subjects (because of reduced compliance and wave reflections), which better indexed the arterial load effects on the ventricle. Simple methods to estimate  $E_a(PV)$  from routine arterial pressures were tested and validated.

**Conclusions.**  $E_a(PV)$  provides a convenient, useful method to assess arterial load and its impact on the human ventricle. These results highlight effects of increased pulsatile load caused by aging or hypertension on the pressure–volume loop and indicate that this load and its effects on cardiac performance are often underestimated by mean arterial resistance but are better accounted for by  $E_a$ . (*Circulation* 1992;86:513–521)

**KEY WORDS** • hypertension • ventricle • afterload • pressure–volume relations

Arterial load is most commonly expressed as mean vascular resistance, a description that ignores the pulsatile nature of both pressure and flow. Under normal circumstances, oscillatory components of arterial load are minor<sup>1–3</sup>; therefore, this characterization is usually adequate. This is less true of human subjects with hypertension and/or vascular aging, in whom pulsatile load becomes increasingly prominent.<sup>4–9</sup> Studies have demonstrated the importance of systolic pressure and pulsatile load as a risk factor for cardiovascular morbidity and mortality<sup>10,11</sup> and for ventricular hypertrophy.<sup>12</sup> As a result, alternatives to mean resistance have been sought. A more precise and complete description is provided by the aortic input impedance

spectra<sup>1,3,13</sup> defined in the frequency domain.<sup>1</sup> Unfortunately, it is very difficult to link such data with time-domain or pressure–volume measurements of ventricular function in order to understand or predict their interaction.<sup>14</sup> Studies that have attempted this<sup>15,16</sup> (using an inverse Fourier transform to derive an impulse response function) are complex and have thus far been relegated to modeling studies.

One approach, first proposed by Sunagawa et al,<sup>17,18</sup> simplifies the arterial load into an effective arterial elastance ( $E_a$ ).  $E_a$  is defined as a steady-state arterial parameter that incorporates the principal elements of vascular load including peripheral resistance, total lumped vascular compliance, characteristic impedance, and systolic and diastolic time intervals. This parameter can also be approximated by the steady-state ratio of end-systolic pressure obtained from the pressure–volume loop divided by stroke volume ( $P_{es}/SV$ ). It is this even simpler approximation that has rendered  $E_a$  so useful in studies of ventricular arterial interaction, because it shares common units with elastance measures of ventricular function<sup>17–24</sup> obtained from pressure–volume relations. However, whereas the  $P_{es}/SV$  ratio has proven suitable in isolated heart or intact animal studies in which vascular systems are either model generated or highly compliant,<sup>17,18,22,24</sup> it remains un-

From the Division of Cardiology, Department of Internal Medicine, Johns Hopkins Medical Institutions, Baltimore, Md., and the Division of Cardiology, Veterans General Hospital, Taipei, Taiwan, ROC.

Supported by Academia Sinica, Taipei, Taiwan; National Heart, Lung, and Blood Institute Physician Scientist grant HL-01820 (D.A.K.); Heart Foundation of Australia; Fulbright Foundation; and Royal Australian College of Physicians (R.P.K.). Dr. Kass is an Established Investigator of the American Heart Association.

Address for correspondence: David A. Kass, MD, Johns Hopkins Medical Institutions, Carnegie 538, 600 N. Wolfe Street, Baltimore, MD 21205.

Received November 7, 1991; revision accepted May 7, 1992.

known whether it applies to real impedances in human subjects with stiffer vasculatures.

The purpose of the present study, therefore, was to test the validity of assessing human vascular loading by  $E_a$  as derived from steady-state pressure–volume data. To achieve this, simultaneous invasive measurements of ventricular pressure–volume and aortic pressure–flow (input impedance) data were obtained in 10 subjects under a variety of loading and pharmacological conditions. Vascular parameters (three-element Windkessel model) were derived from the arterial pressure–flow data and used to determine an effective elastance [ $E_a(Z)$ , the “Z” denotes its derivation from arterial data] characterizing the vascular load. This was then directly compared with the  $P_{es}/SV$  ratio obtained from simultaneous pressure–volume loops [denoted as  $E_a(PV)$ ]. The results reveal an excellent correspondence between the measures and also provide an approach for calculating  $P_{es}$  and thus  $E_a$  from routine arterial pressures.

### Methods

Ten subjects (nine men and one woman) aged 19–60 years were studied in the catheterization laboratories of the Veterans General Hospital, Taipei, Taiwan. Patients were referred for routine diagnostic cardiac catheterization primarily for atypical chest pain. All had normal coronary arteriography and left ventriculography at the time of catheterization. Six older subjects (group A: mean age,  $41 \pm 9$  years) had a history of essential hypertension (controlled by monotherapy), and four younger subjects (group B: mean age,  $21 \pm 3$  years) were normotensive. Chronic medications were held 10 days before study. Informed consent was obtained from each patient; the study protocol was approved by the Human Investigation Committee of the Veterans General Hospital, Taipei, with a similar protocol approved by the Joint Committee on Human Investigation of the Johns Hopkins Medical Institutions.

Patients were premedicated with diazepam (10 mg p.o.). Introducer sheaths were placed in the right femoral artery and vein (8F and 9F, respectively) and the left femoral artery (8F) under 1% lidocaine anesthesia. Ascending aortic pressure and flow were measured at the level of the sinuses of Valsalva using a micromanometer-tipped combination pressure–flow velocity catheter (VPC-673D, Millar Instruments, Houston, Tex.) inserted via the left femoral sheath. This catheter had two manometers, one at the tip and another 5–7 cm proximal and an electromagnetic flow velocimeter 3 cm proximal to the second manometer. The velocity sensor was connected to a flowmeter (model BL-613, Biotronex Laboratories, Kensington, Md.). The flow system provided a flat frequency response up to 23 Hz and was decreased by 3 dB at about 75 Hz. The catheter was placed so the distal micromanometer was in the left ventricular outflow tract. Left ventricular pressure–volume relations were simultaneously determined by conductance (volume) catheter (Webster Labs, Baldwin Park, Calif.) attached to a stimulator/processor (Sigma-5, CardioDynamics, Rijnsberg, The Netherlands) described previously in detail.<sup>25,26</sup> The conductance catheter had a pigtail tip and was positioned over a guide wire to lie at the left ventricular apex. A 3F micromanometer catheter (SPC-330A, Millar Instru-

ments) was then placed within the lumen of the conductance catheter and extended to its distal end.

Micromanometers were presoaked in saline at room temperature for at least 1 hour before study. Both the volume catheter signal and the aortic flow velocity signal at baseline steady state were calibrated to stroke volume derived from a right anterior oblique ventriculogram, using the modified single-plane algorithm of Kennedy et al.<sup>27</sup> Hemodynamic recordings were digitized at a rate of 200 Hz using custom-designed data acquisition and display software, and data were stored on removable magnetic disks for subsequent analysis. To test the validity of the  $P_{es}/SV$  ratio to index vascular properties, impedance and pressure–volume data were measured at baseline and after mechanical and pharmacological load interventions. Mechanical preload reduction was achieved via transient occlusion of inferior vena caval inflow using an intravascular balloon (No. 9168, Cordis, Hialeah, Fla.). Balloon inflation with 15–25 ml  $CO_2$  typically resulted in 34% reduction in left ventricular end-diastolic volume. Pharmacological change was induced in seven subjects (four hypertensive and three normal subjects) using  $\beta$ -blockers (propranolol 1 mg/min to total of 0.15 mg/kg,  $n=3$ ; esmolol 2 mg/kg bolus+200  $\mu$ g/kg/min,  $n=1$ ) or vasodilators (captopril 14 mg,  $n=2$ ; verapamil 10 mg,  $n=1$ ).

### $E_a$ Definitions

Theoretic relations between  $E_a$  and arterial properties as modeled by the three-element Windkessel have been previously described in detail.<sup>17,18</sup> In brief,  $E_a$  is defined by the expression

$$E_a(Z) = R_T / [t_s + \tau(1 - e^{-t_d/\tau})] \quad (1)$$

where  $R_T$  is total mean vascular resistance,  $t_s$  and  $t_d$  are the systolic and diastolic time periods, respectively, and  $\tau$  is the diastolic pressure decay time constant, or the product of peripheral arterial resistance and total capacitance. Equation 1 combines lumped descriptions of vascular load obtained from impedance and arterial waveform analysis into an elastance (units of mm Hg/ml). This ratio is termed  $E_a(Z)$ , designating its calculation from vascular and impedance measurements.

Equation 1 can be simplified as follows. If the diastolic pressure decay time constant is long compared with the diastolic time interval ( $\tau \gg t_d$ ), then the denominator reduces to  $t_s + t_d = T$ , the cardiac cycle length. Thus

$$E_a(Z) \approx R_T / T \quad (2)$$

However,  $R_T$  equals mean arterial pressure ( $P_{mean}$ ) divided by cardiac output, thus

$$E_a(Z) \approx R_T / T = P_{mean} / (CO \cdot T) =$$

$$P_{mean} / (SV \cdot HR \cdot T) = P_{mean} / SV \quad (3)$$

If mean arterial pressure is further approximated by end-systolic pressure ( $P_{es}$ ), one gets

$$E_a(Z) \approx P_{mean} / SV \approx P_{es} / SV = E_a(PV) \quad (4)$$

$P_{es}$  is the pressure at the time of maximal ventricular elastance  $[P(t)/(V(t) - V_o)]_{max}$  for a steady-state pressure–volume loop. If  $E_a(PV)$  is to provide a simpler but

valid means to assess the arterial loading, then it should equal  $E_a(Z)$  derived from the more complex three-element Windkessel model of arterial load (Equation 1). The present study focuses on this correspondence as well as the relation between  $E_a(Z)$  and mean resistance given by Equation 2.

### Data Analysis

Four to five steady-state beats were analyzed under each condition (baseline, lower preload, pharmacological intervention), and the results were averaged. Maximal and minimal arterial pressure defined systolic and diastolic pressures, respectively. Pressure was also measured at the site of aortic valve closure indicated by the incisura. End-systolic pressure was the pressure at maximal ventricular elastance ( $P_{es}/V_{es}$ ). Systolic ejection interval ( $t_s$ ) was measured from the foot of the aortic pressure wave to its incisura, and the diastolic interval was  $t_d = T - t_s$ . The compliance ( $C_a$ ) of the arterial bed was measured by the method reported by Liu et al.<sup>28</sup> This avoids nonlinear curve fitting to the diastolic pressure wave by using the area under the waveform.

Aortic input impedance was measured from simultaneously recorded ascending aortic pressure and flow. Steady-state beats were selected, ensuring that the flow waveform had a nearly flat baseline during diastole. The flow signal was first offset so that the baseline had a mean of zero. It was then integrated, and the area under the curve was set equal to stroke volume determined from the ventriculogram. Pairs of pressure and flow data for each beat were analyzed by discrete Fourier transform. The amplitude (modulus) and phase spectrum of input impedance were calculated by dividing the amplitudes (pressure/flow) and subtracting the phase angles at each harmonic, respectively. The resulting impedance spectra for several beats under each condition were averaged at each harmonic and expressed as a mean and 2 SD. Spurious data arising from flow signal noise were excluded by using only spectral components of flow that were of greater amplitude than that found at baseline during mid-to-late diastole. In addition, impedance data above 12 Hz were not analyzed in accordance with previous experience.<sup>3</sup>

The following parameters were obtained from the impedance spectra: the zero frequency modulus or total resistance ( $R_T$ ), characteristic impedance ( $Z_0$ ) determined from the average of impedance moduli between 5 and 12 Hz. If  $Z_0$  is considered as opposition to pulsatile flow in the absence of wave reflections upstream to arteriolar resistance, then based on a three-element Windkessel model,<sup>29</sup> a measure of arteriolar resistance ( $R_a$ ) distal to this site is equal to  $R_T - Z_0$ . The time constant of diastolic pressure decay is the product of  $R_a \cdot C_a (= \tau)$ . In addition, the amplitude and frequency of the first minimum of impedance modulus ( $|Z|_{min}$  and  $f_{min}$ , respectively) and the value and frequency of the first maximum modulus after  $|Z|_{min}$  ( $|Z|_{max}$  and  $f_{max}$ ) were determined. From  $|Z|_{min}$ ,  $|Z|_{max}$ , and  $Z_0$ , the ratio  $(|Z|_{max} - |Z|_{min})/Z_0$  was used to assess modulus fluctuation about  $Z_0$  as an index of wave reflections.<sup>13</sup> The impedance and arterial waveform-derived parameters were then entered into the right side of Equation 1 to determine  $E_a(Z)$ .

### Statistical Analysis

Correlations between  $E_a(Z)$  versus  $E_a(PV)$  and  $E_a(Z)$  versus  $R_T/T$  were determined by least-squares regression. The effects of mechanical preload reduction on impedance and pressure-volume measures of arterial load were assessed by paired *t* test. Data analysis was performed using custom-developed as well as commercial software, using a 16-bit 386 microprocessor personal computer.

## Results

### Impedance Versus Pressure-Volume Manifestations of Arterial Load

The study patients fell into two groups: Group A patients ( $n=4$ ) were young and normotensive, and group B patients ( $n=6$ ) were older with moderate hypertension. Group B subjects had significantly greater ( $p < 0.05$ ) peak systolic and pulse pressure compared with group A subjects ( $154 \pm 22$  versus  $121 \pm 5$  mm Hg and  $63 \pm 16$  versus  $41 \pm 4$  mm Hg), lower arterial compliance ( $1.0 \pm 0.22$  versus  $1.65 \pm 0.64$  ml/mm Hg), and were twice as old ( $41 \pm 9$  versus  $21 \pm 3$  years).

Figure 1 displays arterial pressure and flow waveforms and pressure-volume loops for typical group A and group B subjects. The young normotensive subject (A, solid line) has a narrow arterial pulse pressure with rounded systolic contour and a high, sharp-peaked, aortic-flow waveform. The corresponding pressure-volume loop (right panel) is square in shape, with little change in systolic pressure from the onset to end of ejection. In contrast, the older, hypertensive subject (B, dashed lines) has a wider pulse pressure, an early pressure inflection, and a late systolic peak. The flow waveform demonstrates a reduced peak and early plateau synchronous with the pressure inflection. The corresponding pressure-volume loop displays a progressive rise in pressure throughout ejection (trapezoid shape). All these characteristics are consistent with reduced arterial compliance and enhanced wave reflections. These data, in particular, are distinctly different from the animal data previously used with validated  $E_a$ . For each pressure-volume loop, a line is shown connecting the end-systolic pressure-volume point to the point at (EDV, 0). This line has an absolute slope equal to  $P_{es}/SV$  and thus provides graphical representation of  $E_a(PV)$ .

Figure 2 displays impedance spectra corresponding to the pressure-flow data of the previous figure. The large zero frequency modulus (mean resistance,  $1,227.9$  dyne  $\cdot$  sec  $\cdot$  cm<sup>-5</sup> for normotensive subject A versus  $2,096.9$  for hypertensive subject B) is not plotted to better demonstrate disparities in higher-frequency terms. The first modulus minimum and zero-phase crossover point occur at a lower frequency for subject A compared with B. In addition, there are greater fluctuations beyond the first modulus minimum and first zero-phase crossing in subject B. All these differences are consistent with an older and stiffer vasculature for the group B patient. It is worth contrasting the relative complexity of the impedance spectra assessment of vascular load as opposed to the simplicity of the  $E_a$  representation shown in Figure 1. It would seem quite beneficial if the dominant mean and pulsatile information embodied in the impedance spectrum could indeed be reflected by this far simpler parameter.

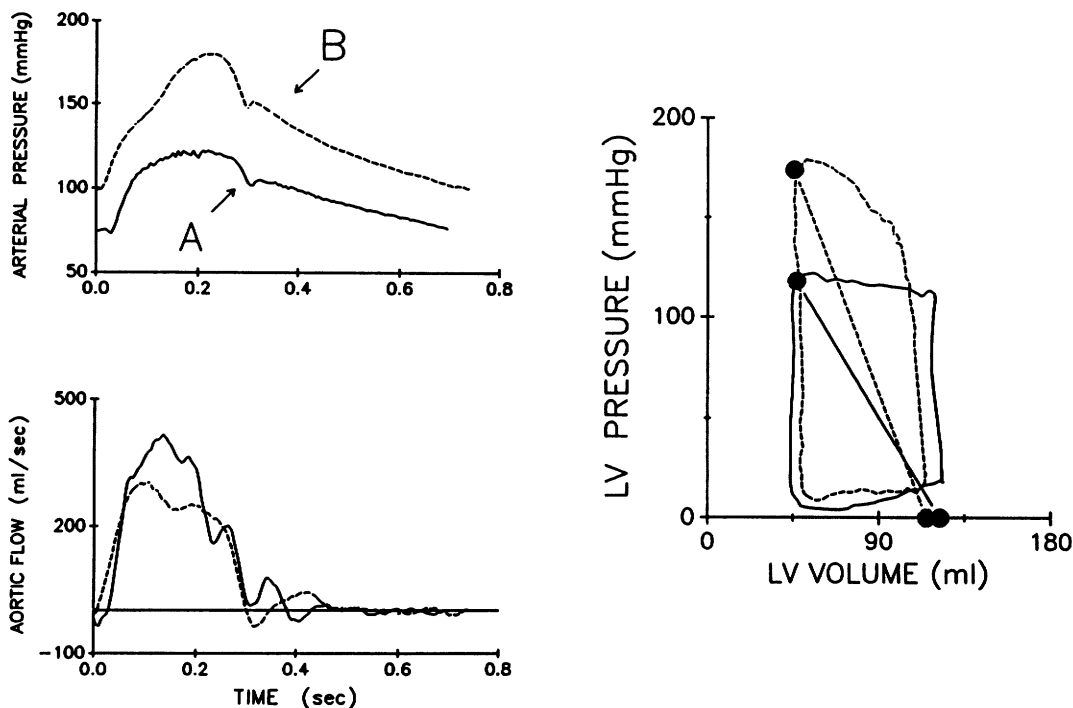


FIGURE 1. Graphs show central arterial pressure (upper left panel) and flow (lower left panel) waveforms and corresponding ventricular pressure–volume loops (right panel) for a young normotensive subject (A, solid lines) versus an older hypertensive subject (B, dashed lines). The group A subject had a narrower pulse pressure, higher and sharper peak flow, and a more square pressure–volume loop compared with the group B subject. Lines representing  $E_a (=P_{es}/SV)$  are shown for each pressure–volume loop. LV, left ventricular. See text for details comparing the two data sets.

#### $E_a(PV)$ Versus $E_a(Z)$

Despite the varying vascular properties in these patients, the ratio of ventricular end-systolic pressure to stroke volume [ $P_{es}/SV = E_a(PV)$ ] was remarkably similar

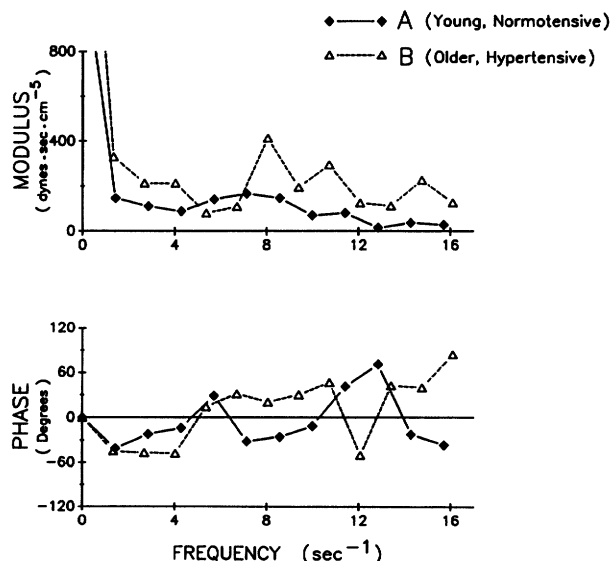


FIGURE 2. Plots show impedance spectra from the same two example subjects displayed in Figure 1. The younger normotensive subject (A) displays an early first impedance minimum and zero-phase crossover and reduced power and oscillations at higher frequencies than the older hypertensive (B) subject.

to  $E_a(Z)$  derived from the vascular impedance parameters from Equation 1. The two elastances were related by  $E_a(PV) = 1.0 \cdot E_a(Z) + 0.16$ ;  $r^2 = 0.96$ ,  $p < 0.0001$  (not significantly different from the line of identity).

To broaden the comparison between the simple (pressure–volume derived) versus more complex (impedance derived) calculation of  $E_a$ , data were obtained at reduced volumes and after pharmacological interventions. Mechanical preload reduction lowered stroke volume by 23%, mean arterial pressure by 21%, and peak systolic pressure by 26% (Table 1). Arterial compliance increased by 75.6% ( $p < 0.001$ ), whereas characteristic impedance decreased by 44% ( $p < 0.001$ ). The impedance analysis demonstrated reduction of moduli at higher frequencies and in the more hypertensive subjects, a leftward frequency shift of first impedance minimum ( $3.5 \pm 0.8$  Hz [group B] versus  $2.3 \pm 0.9$  Hz [group A],  $p < 0.05$ ). These changes are consistent with greater vascular distensibility and reduced wave reflections at lower arterial distending pressures. Interestingly, mean vascular resistance did not change significantly. This contrasts to most prior studies in which load effects on vascular properties have been examined using pharmacological interventions (i.e., nitroglycerin) that can directly affect vascular smooth muscle. In contrast to acute preload reduction, vasodilators (verapamil and captopril) reduced both mean resistance and  $E_a$  by  $\approx 30\%$  ( $p < 0.10$ ), whereas  $\beta$ -blockers increased both parameters by  $\approx 19\%$  ( $p < 0.05$ ).

Combining all the data from baseline, reduced preload, and drug interventions ( $n = 33$ ), the correlation between  $E_a(PV)$  and  $E_a(Z)$  remained excellent, again

**TABLE 1. Effect of Mechanically Reduced Preload on Arterial Pressures and Waveform, Impedance Spectra, and Pressure–Volume Data**

	High preload	Low preload	<i>p</i>
	Mean±SD	Mean±SD	
P <sub>sys</sub> (mm Hg)	142.0±24.9	104.6±24.5	<0.001
P <sub>dia</sub> (mm Hg)	86.0±13.37	70.7±16.0	<0.001
P <sub>inc</sub> (mm Hg)	122.5±20.49	90.28±24.5	<0.001
P <sub>mean</sub> (mm Hg)	111.4±15.97	85.68±19.8	<0.001
P <sub>mej</sub> (mm Hg)	124.8±19.35	94.32±22.6	<0.001
P <sub>es</sub> (mm Hg)	137.4±24.59	98.6±24.8	<0.001
Stroke volume (ml)	71.5±20.2	53.51±21.2	<0.005
Stroke work (mm Hg · ml)	8,011±2,799	5,391±2,745	<0.001
EDV (ml)	123.0±38.2	81.0±35.2	<0.001
R <sub>T</sub> (dyne · sec · cm <sup>-5</sup> )	1,640.0±466.6	1,773.3±520.0	NS
R <sub>a</sub> (dyne · sec · cm <sup>-5</sup> )	1,520.0±426.67	1,706.67±520.0	NS
Z <sub>o</sub> (dyne · sec · cm <sup>-5</sup> )	120.0±53.3	66.7±26.7	<0.001
C <sub>a</sub> (ml/mm Hg)	1.25±0.55	2.10±0.87	<0.001
τ (R <sub>a</sub> · C <sub>a</sub> ) (seconds)	1.31±0.38	2.50±0.69	<0.001
f <sub>min</sub> (sec <sup>-1</sup> )	3.11±0.88	2.23±0.79	<0.10
f <sub>max</sub> (sec <sup>-1</sup> )	7.2±1.13	5.44±1.26	<0.02
Z <sub>lmax</sub> – Z <sub>lmin</sub>  /Z <sub>o</sub>	1.17±0.58	0.62±0.34	<0.05
E <sub>a</sub> (PV) (mm Hg/ml)	2.05±0.57	2.02±0.60	NS
E <sub>a</sub> (Z) (mm Hg/ml)	1.86±0.55	1.92±0.63	NS
R <sub>T</sub> /T (mm Hg/ml)	1.69±0.51	1.80±0.62	NS
P <sub>es</sub> –P <sub>mean</sub> (mm Hg)	26.0±11.7	12.9±8.0	<0.001
P <sub>es</sub> –P <sub>mej</sub> (mm Hg)	12.6±8.4	4.28±5.9	<0.001
E <sub>a</sub> (PV)–R <sub>T</sub> /T (mm Hg/ml)	0.35±0.14 (22%)	0.23±0.12 (14.4%)	<0.001

All data are from all subjects (*n*=10). P<sub>sys</sub>, arterial systolic pressure; P<sub>dia</sub>, arterial diastolic pressure; P<sub>inc</sub>, incisura pressure; P<sub>mean</sub>, mean arterial pressure; P<sub>mej</sub>, mean arterial ejection pressure; P<sub>es</sub>, ventricular end-systolic pressure; EDV, end-diastolic volume; R<sub>T</sub>, total mean resistance; R<sub>a</sub>, estimated peripheral arterial resistance; Z<sub>o</sub>, characteristic impedance; C<sub>a</sub>, total arterial compliance; τ, time constant of diastolic pressure decay; f<sub>min</sub> and f<sub>max</sub>, frequency at first impedance modulus minimum and subsequent maximum, respectively; |Z<sub>lmax</sub>–|Z<sub>lmin</sub>|/Z<sub>o</sub>, arterial reflection index (see “Methods”).

falling along the line of identity (Figure 3). The linear relation was given by E<sub>a</sub>(PV)+0.98 · E<sub>a</sub>(Z)+0.17, *r*<sup>2</sup>=0.98, *p*<0.0001, with a small SEE (0.09 mm Hg/ml).

*E<sub>a</sub>*(PV) Versus R<sub>T</sub>/T

To test the correspondence between E<sub>a</sub> and the more common measure of arterial load, namely mean arterial resistance, we compared E<sub>a</sub>(PV) with the ratio of total mean resistance divided by cardiac cycle length (R<sub>T</sub>/T, see “Methods,” Equation 2). Dividing R<sub>T</sub> by cycle length is required to convert resistance to elastance units. As was true for the relation between E<sub>a</sub>(PV) and E<sub>a</sub>(Z), there was a strong linear correlation between E<sub>a</sub>(PV) and R<sub>T</sub>/T: E<sub>a</sub>(PV)=1.0 · R<sub>T</sub>/T+0.25; *r*<sup>2</sup>=0.96, *p*<0.0001 (Figure 4). However, in this case, E<sub>a</sub>(PV) significantly exceeded R<sub>T</sub>/T at virtually all values. This difference was more notable at baseline or high loads than at reduced loads (i.e., lowered preload or vasodilation). For example, E<sub>a</sub>(PV) exceeded mean resistance (R<sub>T</sub>/T) by 22% at high preload versus only 14.4% at reduced preload (*p*<0.001; see Table 1). The difference between E<sub>a</sub>(PV) and R<sub>T</sub>/T reflected the oscillatory load caused by reduced compliance, increased charac-

teristic impedance, wave reflections, etc., which was lessened by lowering preload.

*E<sub>a</sub> Estimation From Routine Arterial Pressures*

Measurement of E<sub>a</sub> from the P<sub>es</sub>/SV ratio requires determination of end-systolic pressure and stroke volume from a steady-state pressure–volume loop. This is cumbersome for routine or noninvasive clinical assessment. However, the striking linear correlation between E<sub>a</sub>(PV) and R<sub>T</sub>/T suggests that modification of a generally accepted formula for calculating mean arterial pressure might yield a good approximation to E<sub>a</sub>. The difference between P<sub>es</sub>/SV and R<sub>T</sub>/T lies in the discrepancy between P<sub>es</sub> and P<sub>mean</sub> (see Equation 4). P<sub>mean</sub> is frequently estimated by the sum of (P<sub>sys</sub>+2 · P<sub>dia</sub>)/3. We hypothesized that P<sub>es</sub> could be better estimated by reversing the weighing of systolic and diastolic pressures in the expression P<sub>es</sub>≈(2 · P<sub>sys</sub>+P<sub>dia</sub>)/3. Dividing this result by stroke volume, we could approximate E<sub>a</sub>(PV). The results (Figure 5) show this to be correct, with E<sub>a</sub> predicted very well by this simple ratio derived from central aortic pressures (E<sub>a,est</sub>=1.0 · E<sub>a</sub>(PV)–0.16; *r*<sup>2</sup>=0.96, SEE=0.13, *p*<0.0001). End-systolic pressure was also accurately predicted by multiplying peak arte-

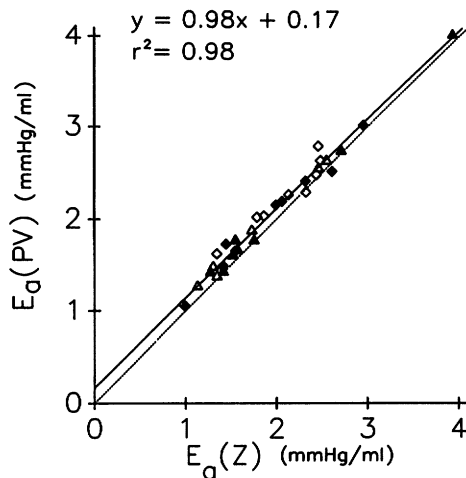


FIGURE 3. Plot shows comparison of effective arterial elastance ( $E_a$ ) derived from vascular impedance analysis [ $E_a(Z)$ ] using Equation 1 in "Methods" versus  $E_a$  derived from the ventricular pressure-volume loop as the ratio of end-systolic pressure to stroke volume [ $E_a(PV)$ ], Equation 4 in "Methods". The two estimates were remarkably similar, with a mean regression slope of 0.98 and offset of 0.17 ( $p < 0.001$ ). This relation was statistically similar to the line of identity (dotted line).

rial systolic pressure ( $P_{\text{sys}}$ ) by 0.9. Again, dividing by stroke volume, one obtains another accurate  $E_a$  estimate:  $0.9 \cdot P_{\text{sys}}/SV = 1.0 \cdot E_a(PV) - 0.11$ ;  $r^2 = 0.97$ ,  $SEE = 0.12$ ,  $p < 0.0001$ .

### Discussion

The major goal of this study was to test whether human vascular load could be meaningfully assessed by the effective arterial elastance determined by the ratio

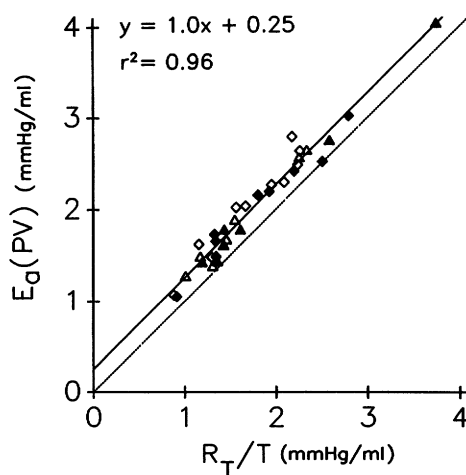


FIGURE 4. Plot shows comparison of  $E_a(PV)$  (effective arterial elastance derived from ventricular pressure-volume loop as ratio of end-systolic pressure to stroke volume) to mean total resistance divided by cardiac cycle length ( $R_T/T$ ).  $E_a(PV)$  was modestly but consistently greater than  $R_T/T$  such that the regression line fell significantly above the line of identity. This disparity represented the influence of pulsatile load.

of end-systolic pressure to stroke volume [ $E_a(PV)$ ]. To achieve this, data were obtained providing simultaneous independent characterizations of arterial load based on arterial pressure-flow and ventricular pressure-volume data. The results confirmed a near identity between the two characterizations over a range of loading and/or pharmacological conditions. The effective arterial elastance consistently exceeded the ratio of mean resistance/cycle length, particularly in older and hypertensive subjects. This indicates an important additional influence of pulsatile impedance load that can be indexed by  $E_a$  but not by steady-state resistance. Finally, a simple estimation formula for end-systolic pressure, and thus  $E_a$ , was tested that makes calculations using routine arterial pressure feasible.

### $E_a$ as Measurement of Vascular Load

$E_a$  was first proposed by Sunagawa et al<sup>17,18</sup> as a means to represent arterial load because it could easily be coupled with ventricular end-systolic pressure-volume relations. This was an important aim, as it enables integrated cardiovascular function variables (cardiac output, stroke work, ejection fraction, efficiency, etc.) to be determined using algebraic ventriculovascular coupling equations.<sup>17-20,22,24,30</sup> The primary assumption was that the vasculature could be reasonably modeled by a three-element Windkessel.<sup>16</sup> Studies performed first in isolated, ejecting canine hearts<sup>17,18,24</sup> and later in intact ventricles<sup>22</sup> confirmed the validity of the theoretical model as well as its value for predicting integrated function variables. However, determination of  $E_a$  from the  $P_{\text{es}}/SV$  ratio required additional simplification of the complex expression (Equation 1) derived from lumped vascular parameters. These assumptions have been shown to be reasonable in isolated heart preparations and normal animals.<sup>16</sup>

The present data extend this to human subjects, both normotensive and hypertensive and young and old. Despite differences between the idealized pressure waveforms used in prior modeling studies and the real human data analyzed in the present study,  $E_a(PV)$  was virtually identical to  $E_a(Z)$ . In "Methods,"  $E_a(Z)$  and  $E_a(PV)$  were related through two assumptions (Equations 2-4):  $P_{\text{es}}$  is approximately equal to  $P_{\text{mean}}$ , and the diastolic decay time constant ( $\tau$ ) is long relative to the diastolic time period (i.e., compliant system). However, in aged or hypertensive subjects, neither assumption holds. This is because the arterial vasculature becomes stiffer or less compliant,<sup>1-9</sup> resulting in a considerable disparity between mean arterial pressure and  $P_{\text{es}}$  but also in shortening of the diastolic decay time constant ( $\tau$ ). The two effects offset one another (see Equation 1) so that  $E_a(Z)$  is still nearly equal to  $E_a(PV)$ . This fact and the persistent high linear correlation between  $E_a(PV)$  and  $R_T/T$  can be best explained if there are relatively few types of vascular property change that naturally occur.<sup>3</sup> Such changes primarily result from lower elasticity leading to a widened pulse pressure and enhanced wave reflections.<sup>4-6</sup>

### Arterial Load and the Pressure-Volume Loop

In adult humans, there are important age-related effects of arterial stiffening on vascular impedance, the arterial pressure wave contour, and pressure-volume loop shape. Although the first two have been well

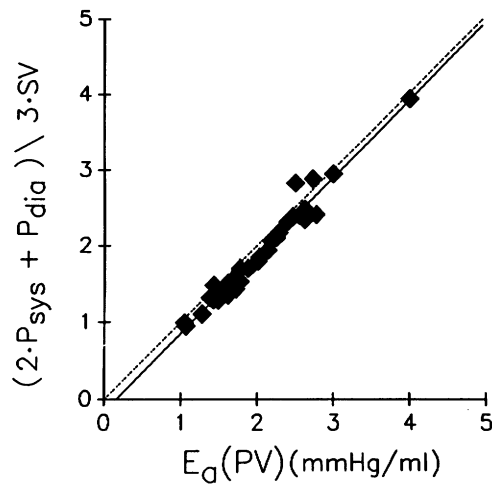


FIGURE 5. Plot shows prediction of  $E_a(PV)$  (effective arterial elastance derived from ventricular pressure–volume loop as ratio of end-systolic pressure to stroke volume) from a simple average of systolic and diastolic arterial pressures. By adding two times the systolic pressure to the diastolic pressure and dividing by 3, (reversing the common weighting used to estimate mean pressure),  $P_{es}$  (end-systolic pressure) and thus  $E_a(PV)$  could be well estimated. The actual regression is shown by the solid line and was not significantly different from the line of identity (dashed line).

documented,<sup>4–7,13</sup> the resultant late-peaking pressure–volume loop has received little attention. Aging results in a progressive rise in aortic late systolic pressure caused by reduced arterial compliance and increased systolic wave reflections<sup>4,8,9,13</sup> and is associated with distinctive changes in aortic input impedance spectra.<sup>3</sup> Loss of arterial elasticity alters both the timing and intensity of wave reflections, and these effects may be amplified in the presence of hypertension.<sup>6</sup> The resulting late peak in aortic pressure is mirrored by a similar rise in ventricular pressure and thus systolic peaking of the pressure–volume loop.

With this in mind, it is instructive to consider the implications of estimating arterial load by  $E_a$  based on end-systolic pressure rather than the mean resistance based on mean arterial pressure. Figure 6 displays pressure–volume loops at baseline and after reduced preload for a young normotensive (panel A) and old hypertensive (panel B) subject, respectively. The end-systolic pressure–volume relations (ESPVRs, solid line) were generated from seven to 10 loops during inferior vena cava occlusion (each with linear correlations  $>0.97$ ). For simplicity, only the loops at upper and lower loads are shown. Each loop intersects the ESPVR at the end-systolic pressure ( $P_{es}$ , solid circles). This largely determines the end of ejection and thus stroke volume and ejection fraction.<sup>22,24</sup> The corresponding arterial pressure traces are shown to the right, and the dashed lines denote the mean pressure value at each respective load (H, high; L, low). For subject A, as in normal animals, there is little disparity between mean arterial pressure and  $P_{es}$ . However, in subject B, there is a considerable difference between the two points. This disparity is greatest at high preload because of the larger influence of pulsatile components. The important

point is that in humans, particularly those with stiff or hypertensive vasculatures, end-systolic pressure and mean arterial pressure can deviate substantially. Yet, as shown in this figure, it is the end-systolic pressure and thus  $E_a$  that better relates the arterial load with ventricular contractile performance (systolic PV boundary) and thus better relates to stroke volume or ejection fraction.

#### Mechanical Versus Pharmacological Load Change

It is well known that arterial distensibility *in vitro* varies with hydraulic load, because as distending pressure rises, a greater proportion of the load is borne by the collagenous rather than elastic components of the arterial wall.<sup>31,32</sup> Previous *in vivo* studies of such load dependency in humans have relied on pharmacological interventions to induce arteriolar constriction or dilation that generally altered mean resistance via direct effects on vascular smooth muscle.<sup>33–36</sup> The present data provide the first quantification of the magnitude of pressure-dependent changes in vascular loading (compliance, characteristic impedance, etc.) independent of potential direct pharmacological actions on vascular smooth muscle. As demonstrated in Table 1, there was no significant change in total or estimated peripheral arterial resistance, whereas compliance, characteristic impedance, and other manifestations of pulsatile load were altered. As recently demonstrated, the stiffer the vasculature, the greater the mean pressure dependence of these pulsatile components.<sup>37</sup>

#### Methods to Measure $E_a$

In the current study, both  $E_a(Z)$  and  $E_a(PV)$  were determined from steady-state arterial impedance or pressure–volume data. This makes sense, because vascular properties are usually measured at steady state under a given range of distending pressure. Furthermore, the original derivation of  $E_a$  from vascular parameters<sup>17</sup> (Equation 1) assumes measurements of resistance, characteristic impedance, and lumped compliance at steady state. Several recent animal and clinical studies using this parameter have derived  $E_a$  from the slope of a linear relation between  $P_{es}$  and stroke volume over a preload range.<sup>19,20</sup> This is a more complicated approach that stems from a conceptual model of ventricular–vascular coupling also described by Sunagawa et al.<sup>17</sup> However, inherent in this relation are assumptions that the vascular properties are fixed and thus independent of mean distending pressure, and the data are obtained at steady state. These assumptions are rarely true *in vivo* as shown in Table 1. Derivation of  $E_a$  from the ratio of  $P_{es}/SV$  ultimately involves fewer assumptions and can be directly related to vascular impedance load at steady state. The present study further demonstrates how this ratio can be more simply estimated using resting arterial systolic and diastolic pressures as shown in Figure 5.

#### Limitations

This study reports data from a fairly small subject group. However, the use of precise simultaneous measurements and varying load conditions provided sufficient data for meaningful regression analysis. Furthermore, the regression analysis displayed little scatter, suggesting that additional patients probably would not alter the results. Volume calibration was based on

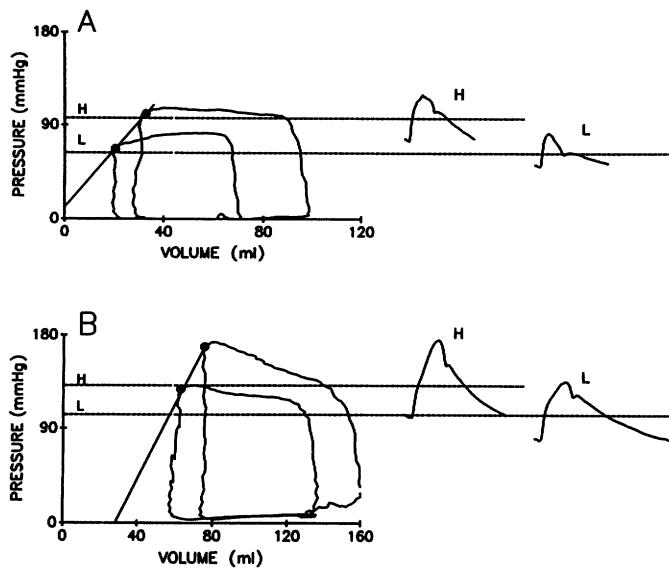


FIGURE 6. Graphs show disparity of estimating the effect of arterial load on ventricular function using mean arterial pressure (and thus mean resistance) versus end-systolic pressure (and thus, effective arterial elastance,  $E_a$ ). Two pressure-volume loops are displayed in a young normotensive (panel A) and older hypertensive (panel B) subject at baseline and reduced preload. The end-systolic pressure-volume relation (solid line) was obtained from seven to 10 intervening beats (not displayed for simplicity). End-systolic pressure-volume points are shown by solid circles. Simultaneous arterial pressure waveforms and their respective means (dashed lines) are also shown for both high (H) and low (L) volume beats. See text for details.

ventriculography, which can be subject to error. However, most of the analysis required only that the same calibration be applied to both ventricular and vascular parameter data. Thus, volume calibration errors would have little effect on the comparisons between  $E_a(PV)$  versus  $E_a(Z)$  or high- versus low-preload impedance data.

The  $E_a$  data from older hypertensive subjects represents a clear departure from previously reported animal validation data because of the greater pulsatile load. However, the study group did not include extremes of hypertension- or age-related vascular changes that can occur. Arterial systems poorly described by lumped models such as the three-element Windkessel (i.e., those with very marked systolic wave reflections and wave transmission effects) may also be inadequately represented by  $E_a$ . Having stated this, it should be noted that the data collected did span a wide range of systolic pressures (180.1–73.3 mm Hg) and resistances. The near equivalency of both  $E_a(Z)$  and  $E_a(PV)$  over this full range supports its use under many clinical conditions.

In addition to vascular impedance load,  $E_a$  also incorporates heart rate information (see Equations 1 and 2). One can argue that inclusion of cycle length in a parameter meant to estimate arterial load is problematic, because the measurement is thus sensitive both to vascular and cardiac properties. However, heart rate is an important determinant of cardiac pump performance, and an increase in rate can have similar effects (increasing the  $P_{es}/SV$  ratio) as an increase in resistance. This change is understandable in light of the shortened diastolic decay period and thus higher mean pressure during tachycardia. Heart rate dependence of  $E_a$  has recently been used to distinguish inotropic effects of pacing tachycardia from dobutamine stimulation.<sup>38</sup>

### Conclusions

Recent studies have stressed the importance of abnormal pulsatile load effects on cardiac function, energetics, cardiac hypertrophy, and the physiology of aging.<sup>4,7,10–12,36</sup> Simple methods to assess this load have been sought, including pulse waveform and impedance analysis.<sup>1,3,13</sup> In the present study, we demonstrated that

the ratio of end-systolic pressure to stroke volume [ $E_a(PV)$ ] can also index this load, with the additional and considerable advantage that it is easily linked to measures of ventricular chamber function. Our analysis also provides a method to approximate  $E_a$  from routine arterial pressure recordings, thereby removing requirements for more complex pressure-volume relation analysis. We would anticipate that this load estimate, particularly in older or exercising subjects, will be valuable because of its more direct relation to systolic chamber performance.

### References

- Nichols W, O'Rourke M: Vascular impedance, in *McDonald's Blood Flow in Arteries*. London, Edward Arnold, 1990, pp 283–329
- O'Rourke MF: Steady and pulsatile energy losses in the systemic circulation under normal conditions and in simulated arterial disease. *Cardiovasc Res* 1967;1:313–326
- Murgo JP, Westerhof N, Giolma JP, Altobelli SA: Aortic input impedance in normal man: Relationships to pressure waveforms. *Circulation* 1980;62:105–116
- Nichols WW, O'Rourke MF, Avolio AP, Yaginuma T, Murgo JP, Pepine CJ, Conti CR: Effects of age in ventricular/vascular coupling. *Am J Cardiol* 1985;55:1179–1184
- Avolio AP, Chen SG, Wang RP, Zhang CL, Li MF, O'Rourke MF: Effects of age on changing arterial compliance and left ventricular load in a northern Chinese urban community. *Circulation* 1983;68:50–58
- Merillon JP, Fontenier GJ, Larallut JF, Jaffrin MY, Motte CA, Genain GP, Gourgon RR: Aortic input impedance in normal man and arterial hypertension: Its modification during changes in aortic pressure. *Cardiovasc Res* 1986;16:646–656
- Nichols WW, O'Rourke MF: Aging, high blood pressure and disease in humans, in *McDonald's Blood Flow in Arteries*, ed 3. London, Edward Arnold, 1990, pp 398–420
- Murgo JP, Westerhof N: Arterial reflections and pressure waveforms in humans, in Yin FCP (ed): *Ventricular/Vascular Coupling*. New York, Springer-Verlag, 1987, pp 140–158
- Avolio AP, Deng FQ, Li WQ, Luo YF, Huang ZD, Xing LF, O'Rourke MF: Effects of aging on arterial distensibility in populations with high and low prevalence of hypertension: Comparison between urban and rural communities in China. *Circulation* 1985;71:202–210
- Rutan GH, Kuller LH, Neaton JD, Wentworth DN, McDonald RH, McFate-Smith W: Mortality associated with diastolic hypertension and isolated systolic hypertension among men screened for Multiple Risk Factor Intervention Trial. *Circulation* 1988;77:504–514

11. Kannel WB, Wolf PA, McGee DL, Dawber TR, McNamara P, Castelli WP: Systolic blood pressure, arterial rigidity, and risk of stroke. *JAMA* 1981;245:125-129
12. Pearson AC, Gudipati C, Nagelhout D, Sear J, Cohen JD, Labovitz AJ: Echocardiographic evaluation of cardiac structure and function in elderly subjects with isolated systolic hypertension. *J Am Coll Cardiol* 1991;17:422-430
13. Nichols WW, Conti CR, Walker WE, Milnor WR: Input impedance of the systemic circulation in man. *Circ Res* 1977;40:451-458
14. Latson TW, Yin FCP, Hunter WC: The effects of finite wave velocity and discrete reflections on ventricular loading, in Yin FCP (ed): *Ventricular/Vascular Coupling*. New York, Springer-Verlag, 1987, pp 334-383
15. Latson TW, Hunter WC, Burkhoff D, Sagawa K: Time sequential prediction of ventricular-vascular interactions. *Am J Physiol* 1986; 251:H1341-H1353
16. Burkhoff D, Alexander J, Schipke J: Assessment of Windkessel as a model of aortic input impedance. *Am J Physiol* 1988;255(*Heart Circ Physiol*):H742-H753
17. Sunagawa K, Maughan WL, Burkhoff D, Sagawa K: Left ventricular interaction with arterial load studied in isolated canine ventricle. *Am J Physiol* 1983;56:586-595
18. Sunagawa K, Maughan WL, Sagawa K: Optimal arterial resistance for the maximal stroke work studied in isolated canine left ventricle. *Circ Res* 1985;56:586-595
19. Asanoi H, Sasayama S, Kameyama T: Ventriculoarterial coupling in normal and failing heart in humans. *Circ Res* 1989;65:483-493
20. Kameyama T, Asanoi H, Ishizaka S, Sasayama S: Ventricular load optimization by unloading therapy in patients with heart failure. *J Am Coll Cardiol* 1991;17:199-207
21. Kass DA, Maughan WL: From 'E<sub>max</sub>' to pressure-volume relations: A broader view. *Circulation* 1988;77:1203-1212
22. Kass DA, Grayson R, Marino P: Pressure-volume analysis as a method of quantifying simultaneous drug (amrinone) effects on arterial load and contractile state in vivo. *J Am Coll Cardiol* 1990; 16:726-732
23. Latham RD, Rubal BJ, Sipkema P, Westerhof N, Virmani R, Robinowitz M, Walsh RA: Ventricular/vascular coupling and regional arterial dynamics in the chronically hypertensive baboon: Correlation with cardiovascular structural adaptation. *Circ Res* 1988;63:798-811
24. Kass DA, Maughan WL, Guo ZM, Kono A, Sunagawa K, Sagawa K: Comparative influence of load versus inotropic states on indexes of ventricular contractility: Experimental and theoretical analysis based on pressure-volume relationships. *Circulation* 1987;76:1422-1436
25. Kass DA, Yamazaki T, Burkhoff D, Maughan WL, Sagawa K: Determination of left ventricular end-systolic pressure-volume relationships by the conductance (volume) catheter technique. *Circulation* 1986;73:586-595
26. Kass DA, Midei M, Graves W, Brinker JA, Maughan WL: Use of a conductance (volume) catheter and transient inferior vena caval occlusion for rapid determination of pressure-volume relationships in man. *Cathet Cardiovasc Diagn* 1988;15:192-202
27. Kennedy JW, Trenholme SE, Kosser IS: Left ventricular volume and mass from single-plane cineangiogram: A comparison of anteroposterior and right anterior oblique methods. *Am Heart J* 1970;80:343-352
28. Liu Z, Brin KP, Yin FCP: Estimation of total arterial compliance: An improved method and evaluation of current methods. *Am J Physiol* 1986;251:H588-H600
29. Sunagawa K, Maughan WL, Sagawa K: Stroke volume effect of changing arterial input impedance over selected frequency ranges. *Am J Physiol* 1985;248:H477-H484
30. Burkhoff D, Sagawa K: Ventricular efficiency predicted by an analytical model. *Am J Physiol* 1986;250:R1021-R1027
31. Bergel DH: The static elastic properties of the arterial wall. *J Physiol (Lond)* 1961;156:445-457
32. Learoyd BM, Taylor MG: Alterations with age in the visco-elastic properties of human arterial walls. *Circ Res* 1966;18:278-292
33. Yaginuma T, Avolio AP, O'Rourke MF, Nichols WW, Morgan JJ, Roy P, Baron D, Branson J, Feneley M: Effect of glyceryl trinitrate on peripheral arteries alters left ventricular hydraulic load in man. *Cardiovasc Res* 1986;20:153-160
34. Fitchett D, Simkus G, Beaudry J, Marpole D: Reflected waves in the ascending aorta: Effect of glyceryl trinitrate. *Cardiovasc Res* 1988;22:494-500
35. Gundel W, Cherry G, Rajagopalan B, Tan LB, Lee G, Schultz D: Aortic input impedance in man: Acute response to vasodilator drugs. *Circulation* 1981;63:1305-1314
36. Merillon JP, Fontenier G, Larallut JF, Jaffrin MY, Chastre J, Assayag P, Motte G, Gourgon R: Aortic input impedance in heart failure: Comparison with normal subjects and its changes during vasodilator therapy. *Eur Heart J* 1984;5:447-455
37. Carrol JD, Shroff S, Wirth P, Halsted M, Rajfer S: Arterial mechanical properties in dilated cardiomyopathy. *J Clin Invest* 1991;87:1002-1009
38. Freeman G: Role of ventriculovascular coupling in cardiac response to increased contractility in closed-chest dogs. *J Clin Invest* 1990;86:1278-1284